

<https://doi.org/10.1038/s40494-025-01854-0>

Developing a color discrimination model for heritage apparel and accessories based on computational algorithms

**Yu Zhao^{1,3}, Yan Cheng^{1,3}, Yuxiang Zhang¹ & Yi Xiang²**

Heritage apparel and accessories embody the culture, history and aesthetics of certain region or nation, and their colors reflect profound social level, religious belief and lifestyles of the wearers. However, existing studies on their colors are fragmented and inefficient, leading to a limited understanding of their color characteristics and hindering deeper insight into the culture behind. To address these challenges, this study has developed an advanced color discrimination model for heritage apparel and accessories based on computational algorithms and introduce Bonpo apparel and accessories as case study to validate the model. By applying the Fuzzy C-Means (FCM) algorithm, the Elbow method, and Gaussian Mixture Model (GMM), this model systematically captures and discriminates key color characteristics, including color ratios, LAB color space, Euclidean distance, and color co-occurrence frequency. This systematic color discrimination model for heritage apparel and accessories that can be employed for both further studies and new designs.

Heritage apparel and accessories refers to traditional clothing and its adornments passed down through generations, serving as significant carrier of intangible cultural heritages, such as national identities, regional customs, history, and so on¹. Their colors are not merely decorative elements but reflect profound social levels, religious belief, and lifestyles of the wearers. For instance, in ancient China, bright yellow was exclusively used for imperial garments, while commoners were forbidden from wearing it, reinforcing the class system²; Tibetan Buddhist monks wear robes primarily in red and yellow, symbolizing wisdom, ascetic practice, and purification³; The traditional Djellaba in the coastal areas of Morocco are commonly light blue and white, reflecting the Mediterranean aesthetic and a sense of freshness⁴. In addition, the colors of heritage apparel and accessories play a key role in the implementation of heritage restoration, museum display, and modern design. In particular, some ancient apparel and accessories have lost their original vibrancy over time, and accurate color characteristics can help experts restore them by matching the original hues⁵. Nowadays, many museums have conducted digital reconstructions of the heritage apparel by establishing its dynamic 3D models, which also requires specific color characteristics⁶. Besides, when creating the modern apparel design, the colors characteristics of heritage apparel are important reference for its classic coloration and elegant vibe⁷. Therefore, the accurate the color characteristics of heritage apparel and accessories can be discriminated, the better they can be preserved and inherited.

Generally, there are a few color characteristics of heritage apparel and accessories. First, the color composition of heritage apparel and accessories varies widely. Some apparel and accessories feature monochromatic schemes, where similar hues dominate, making color discrimination challenging⁸. Others adopt polychromatic schemes, with distinct contrasting colors, facilitating easier discrimination⁹. For example, the heritage apparel of the Bedouin people primarily consists of earthy tones such as deep brown, beige, and red¹⁰, creating a typical example of color similarity within the same color family, which causes trouble in color discrimination, especially in historical or low-resolution images¹¹. In contrast, the Tuareg people's deep blue robes paired with white turbans create a strong visual distinction¹², reducing the challenges associated with color similarity. Moreover, the resources regarding the color of heritage apparel and accessories often limited in faded, aged, and historical images, making color discrimination challenging¹³.

Existing studies about color discrimination for heritage apparel and accessories primarily adopt descriptive or computational approaches. Regarding descriptive approaches, Kvaerne reviewed ancient texts indicating that yellow has been widely applied in Bonpo hats, but there is no clue that which kind of yellow it is¹⁴. Zhao conducted field research and select a few images of Ningbo gold, silver, and color embroidery to analyze the color composition, but ignoring comprehensiveness regarding the color diversity of Ningbo embroidery¹⁵. Cho photographed and recorded the process of creating embroidered rear skirt panels to figure out the colors prefer to be used by Miao women, but no any information shows the dominated color¹⁶.

¹College of Sericulture, Textile and Biomass Sciences, Southwest University, Chongqing, China. ²School of Design and Innovation, China Academy of Art, Hangzhou, China. ³These authors contributed equally: Yu Zhao, Yan Cheng. e-mail: xyxyxiangyi@163.com

Although these studies provide valuable qualitative insights into heritage apparel and accessories' colors, they often rely on manual observation or traditional classification methods, such as historical text interpretation and descriptive image analysis, which are inefficient for processing large-scale datasets. Moreover, these studies frequently lack rigorous quantitative analysis, relying instead on subjective visual assessments or expert judgments, leading to potential inaccuracies.

A computational algorithm is realized in the form of a computational process to discriminate the colors, which fix the problems of efficiency and accuracy to some extent. For monochromatic schemes, Caelin applied the K-means algorithm to discriminate red dye mixtures in woolen historical textiles, but the method proved effective only for single-color samples, limiting its applicability to broader datasets¹⁷. Similarly, Kaplan proposed a color image processing technique to differentiate natural-indigo-dyed fabrics from synthetic alternatives but restricted analysis to only two categories (light blue and deep blue), insufficient for distinguishing a wider spectrum of colors¹⁸. For polychromatic schemes, Dorozyński utilized deep learning (DL) algorithms to analyze European silk textiles, achieving high accuracy but requiring an extensive dataset of 80,880 images, which is impractical for historical garments with limited samples¹⁹. Zhao et al. applied K-means clustering to analyze the color characteristics of Yi costumes but arbitrarily selected the number of clusters, potentially leading to inaccuracies²⁰. Cerrillo-Cuenca used Gaussian Mixture Models (GMM) to emphasize color separation of rock paintings with RGB and LHCUV (Luminance, Hue, Chroma) imagery²¹. Intharah proposed the GMM to segment characters from mural images automatically by discriminate the colors and detect the edges of the characters²². Zhou applied GMM to recognize, segment, and restore the color details of mural images²³. The colors of rock paintings and mural in these studies both appear to be monochromatic, and located in a certain small region with limited dataset, and GMM well manage these situations. It is noted that GMM offer a more common, flexible, and data-driven approach to color discrimination and overcome several limitations of the aforementioned algorithms. Regarding the problem of the suboptimal results of predetermined clusters, GMM offers flexibility in determining the number of clusters instead of assuming spherical clusters, offering a more advanced soft clustering approach. Regarding the requirement of both smaller and large-scale projects, GMM accommodates datasets of varying sizes²⁴. Even though GMM has not yet been quite applied in the heritage apparel and accessories, it is potential to deal with the color discrimination in this area.

In this paper, the study aims to address the issues of inefficiency, inaccuracy, and unsystematic discrimination of colors in heritage textile and accessories. In order to do so, more suitable computational algorithms were applied to develop a color discrimination model. This model was designed to be applied in both small and large scale of the dataset and scenarios where monochromatic and polychromatic color schemes were both available. These images can be collected as clear and many as possible from various places, such as personal photographs or collected from papers, books, or multiple online resources. Particularly, the model can be used in both academic research related to heritage studies of apparel and accessories, as well as in practical applications for the preservation and restoration of heritage apparel and accessories. The rest of the paper is organized as follows: the second section is the methodology for developing the color discrimination model. The third section interprets the results. The last section is the discussion.

Methods

The research framework of the methodology consists of two main phases regarding the model development and the case study. For the model development, it integrates two steps regarding data process with Bigjpg, PS, and FCM, and the data analysis with the Elbow method and GMM. For the case study, it includes two steps regarding the application of the developed model and model validation. The overall research frame work is demonstrated in Fig. 1.

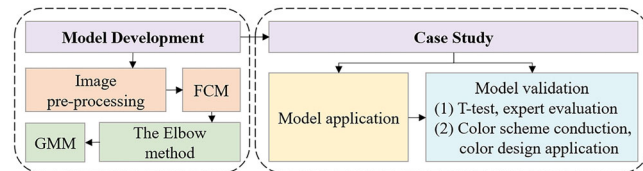


Fig. 1 | The overall research framework of the methods.

Color discrimination model development

To collect the images of heritage apparel and accessories as input data, methods as literature review and field investigation are conducted for collecting images. For the former one, books, articles, and online sources are looked up, and images for heritage apparel and accessories can be collected. In particular, the images collected from literature review are most complete and undamaged among existing remains. For the latter one, images are collected by photographing heritage apparel and accessories wearing by certain wears' like minority groups in various contexts.

Images collected from books, articles, online sources, and museum photographs often show some information loss, including color distortion and low pixel resolution²⁵. This information loss is due to either the quality of the original images or improper photography²⁶. To ensure that the collected images are standardized therefore the model's robustness, preprocessing steps are implemented to address variations in lighting, resolution, and image clarity. Particularly, Both AI-powered and manual methods are employed to preprocess the input collected images and output the optimal ones. AI-powered one offers high precision and efficiency for the image restoration, and the manual method can deal with the images that require complex adjustments, such as correcting intricate details or addressing characteristics that AI may overlook²⁷. In this study, Bigjpg program as an AI-powered method and Adobe Photoshop as a manual tool are applied. Bigjpg program features deep learning algorithms analyzing the textures, colors, and details of the damaged images and performs tasks such as scratch removal, missing area reconstruction, and noise reduction to improve the image quality. Photoshop is applied to deal with certain colors deviating from intended appearance. The original collected images of the heritage apparel and accessories are introduced in the Bigjpg program as input to automatically improve the quality of the images, then being optimized by Photoshop and output to be quality-improved images.

Even though the aforementioned images are preprocessed, they may contain complex backgrounds that display various environmental colors. These complexities may impact the color discrimination results by incorporating background colors into the analysis. Thus, the preprocessed data are fed into the Fuzzy C-Means (FCM) algorithm as input in this study in order to segment the images of heritage apparel and accessories, isolating main regions, and output images with apparel and accessories dominating. FCM algorithm is a well-used unsupervised algorithm based on fuzzy theory, and it was selected for its ability to assign a degree of membership to each pixel across multiple clusters, offering flexibility when processing images with blurred boundaries, especially for heritage apparel with colorful fabrics and faded regions^{28–31}. The objective function of the FCM algorithm is defined as:

$$J = \sum_{i=1}^C \sum_{j=1}^n \sum_{k=1}^d u_{ijk}^\alpha ||x_{jk} - C_{ik}||^2 \quad (1)$$

Here, $||x_{jk} - C_{ik}||^2$ denotes the distance between the k^{th} component of the j^{th} pixel and the corresponding component of the i^{th} cluster center. u_{ijk} denotes the membership degree of pixel x_{jk} to cluster k . C_{ik} denotes the Centroid of cluster k . The parameter $\alpha > 1$ controls the degree of fuzziness. The algorithm is subject to the following constraint:

$$\sum_{i=1}^C \sum_{k=1}^d u_{ijk}^\alpha = 1; j = 1, 2, 3, \dots, n \quad (2)$$

Using the Lagrange multiplier method, the cluster centers and new membership functions are updated iteratively:

$$C_{ik} = \frac{\sum_{j=1}^n u_{ijk}^\alpha x_{jk}}{\sum_{s=1}^n u_{isk}^\alpha}; i = 1, 2, 3, \dots, c; k = 1, 2, 3, \dots, d \quad (3)$$

$$u_{ijk} = \frac{1}{\sum_{h=1}^d \sum_{s=1}^c \left(\frac{d_{sjh}}{d_{sjk}}\right)^{\frac{2}{(\alpha-1)}}}; j = 1, 2, 3, \dots, n \quad (4)$$

After completing these steps, the membership values of each pixel across all components are summed to obtain:

$$u_{ij} = \sum_{k=1}^d u_{ijk} \quad (5)$$

The algorithm iterates the membership values until the difference between consecutive iterations for both samples x_j and cluster centers C_i falls below a predefined error threshold, indicating convergence to an optimal solution. Once the convergence criteria are met, the algorithm terminates and outputs the segmented image.

In order to develop the color discrimination model for heritage apparel and accessories, color cluster is essential to be conducted, and the determination of number for color clusters becomes critical. The Elbow method provides a data-driven mechanism for determining the optimal number of clusters k . This prevents both under and over clustering, which is especially important when analyzing highly diverse and visually complex apparel and accessories, and it is proved to be effective when combining with GMM³²⁻³⁵. In particular, it evaluates the sum of squared errors (SSE) across different k values to determine through the segmented images as input, where adding more clusters yields diminishing improvements in segmentation. This ensures that all meaningful colors are identified without introducing unnecessary complexity or noise³⁶. The SSE is calculated as:

$$\text{SSE} = \sum_{i=1}^k \sum_{x \in C_i} \|x - \mu_i\|^2 \quad (6)$$

where C_i is the set of points in the i th cluster, and μ_i is the centroid of that cluster, and k is the number of clusters being evaluated. As the number of clusters increases, the SSE decreases. The optimal k is determined by identifying the “elbow point” in the SSE curve, where the decrease begins to flatten. This balance helps capture both dominant and subtle colors found in various layers of heritage apparel and accessories.

GMM was chosen over other methods for its capacity to model non-spherical and overlapping color distributions, typical in heritage apparel and accessories imagery. The soft assignment and probabilistic framework make GMM better suited to identify nuanced hues and subtle chromatic variations. It can cluster the main colors and their color characteristics of the heritage apparel and accessories as output through the segmented images as input, according to the clusters k determined by the Elbow method³⁷. The GMM assumes that the dataset follows a mixture of k Gaussian distributions, where each distribution represents a color cluster. Initially, the image data are transformed into the RGB color space, where each pixel x_i is represented by its red, green, and blue components. The initial parameters, including the means μ_i , covariance matrices \sum_i , and mixing coefficients π_i , are set. The clustering process uses the Expectation-Maximization (EM) algorithm. During the E-step, the posterior probability γ_{ij} for each pixel x_i belonging to cluster j is calculated as follows:

$$\gamma_{ij} = \frac{\pi_j N(x_i | \mu_j, \sum_j)}{\sum_{k=1}^K \pi_k N(x_i | \mu_k, \sum_k)} \quad (7)$$

where $N(x_i | \mu_k, \sum_j)$ denotes the probability density function of a Gaussian distribution with mean μ_j and covariance matrix \sum_j . In the M-step, these probabilities were used to update the parameters:

$$\mu_j = \frac{\sum_{i=1}^n \gamma_{ij} x_i}{\sum_{i=1}^n \gamma_{ij}}, \sum_j = \frac{\sum_{i=1}^n \gamma_{ij} (x_i - \mu_j)(x_i - \mu_j)^T}{\sum_{i=1}^n \gamma_{ij}}, \pi_j = \frac{\sum_{i=1}^n \gamma_{ij}}{n} \quad (8)$$

where n is the total number of pixels. These steps are repeated until the change in the log-likelihood function fell below a predefined threshold, indicating convergence. It is noted that depending on the complexity and variety of colors, the number of GMM clustering can be increased. The initial GMM clustering can be performed to capture the color characteristics specific to a single image. The subsequent clustering can be applied to determine the main colors among a set of images. The determination of the number of clusters k in the subsequent clustering can be simplified, such as by employing expert panel and so on. Once the GMM clustering is completed, the results of regular color spaces as RGB and HSV regarding each cluster can be calculated. Furthermore, the more characteristics of color ratios, the LAB color space, color Euclidean distance, and color co-occurrence frequency were calculated based on the determined RGB so as to unify the color space.

Color ratio refers to the proportion of different colors present in the images, reflecting the composition of the items. The color ratios were computed to determine the proportion of pixels in each cluster, calculated as:

$$\text{Ratio}_j = \frac{\text{Number of pixels in cluster } j}{\text{Total number of pixels}} \quad (9)$$

The LAB color space is a color model based on human visual perception, dividing colors into three components, which is lightness (L^*), the red-green opponent channel (a^*), and the yellow-blue opponent channel (b^*). To further explore the characteristics of the clustered colors, they were mapped to the LAB color space based on the RGB values that were calculated before, offering insights into their distribution in terms of lightness (L^*), green-red (a^*), and blue-yellow (b^*) channels³⁸.

Color Euclidean distance refers to the straight-line distance between two color points in a multidimensional color space based on the principles of Euclidean geometry. The similarity between colors is measured using this Euclidean distance in the RGB space:

$$d_{ij} = \sqrt{(R_i - R_j)^2 + (G_i - G_j)^2 + (B_i - B_j)^2} \quad (10)$$

where R_i, G_i, B_i are the color components of cluster i . Smaller distances indicated higher similarity between clusters. Color co-occurrence frequency helps to understand the relationship between colors in the images. It represents how often pairs of colors appear adjacent to each other. The co-occurrence frequency between color clusters and is defined as:

$$C_{ij} = \frac{\text{Number of adjacent pixel pairs with colors } i \text{ and } j}{\text{Total number of adjacent pixel pairs in the images}} \quad (11)$$

By considering the color characteristics of color ratios, LAB color space, Euclidean distances, and co-occurrence frequencies, a detailed understanding of the color discrimination for heritage apparel and accessories can be achieved as the outputs of the proposed color discrimination model.

Model application with Bonpo apparel and accessories

In order to validate the model, this study conducts a case study on Bonpo apparel and accessories. Bonpo apparel and accessories are traditional garments associated with the indigenous Bon religion in Tibet (Xizang), reflecting history and cultural identity. These garments feature a complex color palette including monochromatic hues such as red and brown, and polychromatic hues like blue and yellow. This allows for the simultaneous

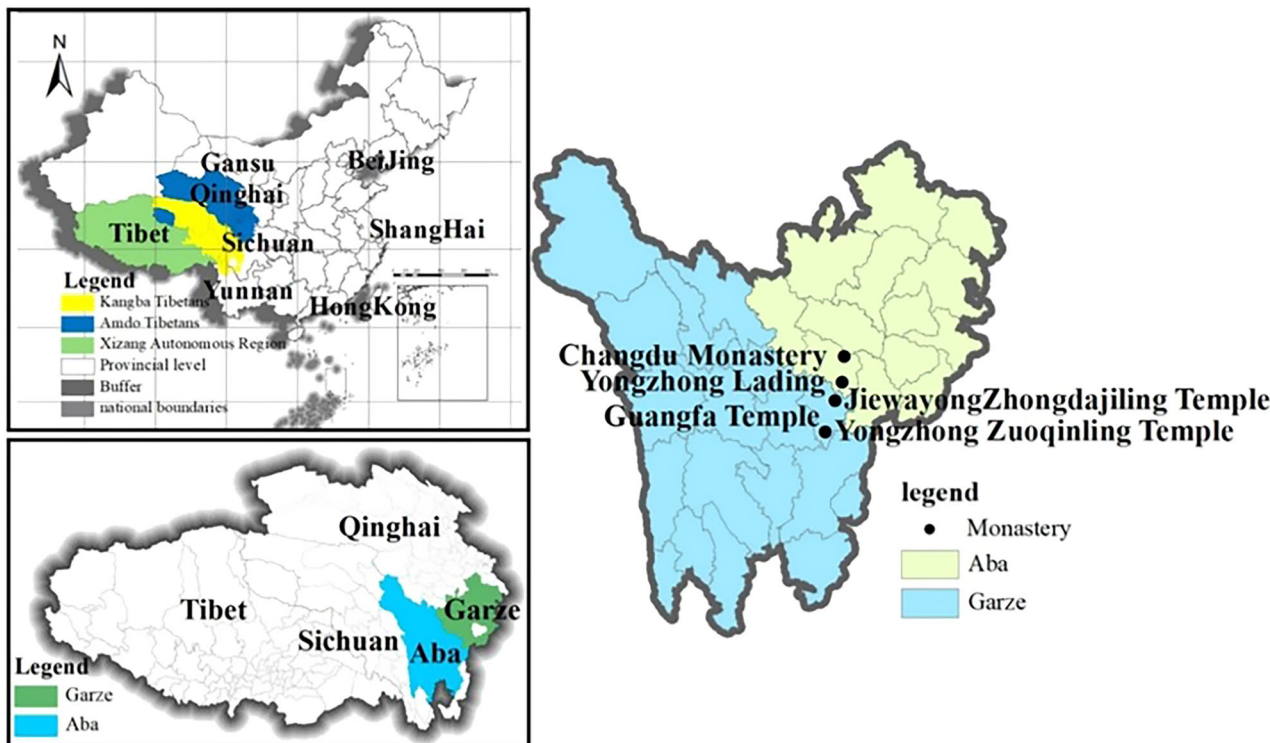


Fig. 2 | Location of remnants of Bonpo apparel and accessories.

evaluation of the model's ability to distinguish between similar and contrasting colors. Moreover, due to the historical decline of the Bon religion and the aging of physical artifacts, very few original Bonpo garments have been preserved. As a typical example of heritage apparel and accessories, Bonpo apparel and accessories present challenges in color discrimination using conventional methods. Therefore, using it as a case study provides a more effective way to evaluate the model's performance.

To apply the proposed model to Bonpo apparel and accessories, this study investigates the Changdu Monastery, Yongzhong Lading, Guangfa Temple, Yongzhong Zuopinlin Temple, and Jiewayong Zhongdajiling Temple (Fig. 2) areas of U-Tsang, Amdo, and Kham in China³⁹, where Bonpo apparel and accessories are mainly distributed. Moreover, images also are collected from Bon museums in these areas. Since the color discrimination model in this study is mainly to discriminate the colors among many colors from every single piece of Bonpo apparel or accessory, images that have single-color apparel and accessory are ought to be removed to ensure that the color discrimination model could effectively analyze a range of co-occurring colors within each image. This can avoid a disproportionate representation of single-color features in the dataset and further focus on images where multiple colors could be analyzed for their relationships and characteristics.

Once the images are obtained, AI-powered and manual methods will be applied for preprocessing, which includes scratch removal, missing area reconstruction, and noise reduction to enhance image quality. After preprocessing, the Fuzzy C-Means algorithm is employed to segment the images, effectively separating the Bonpo apparel and accessories from the background while improving the quality of the segmented regions. To determine the optimal number of clusters for color segmentation, the elbow method is applied to estimate the appropriate k value. The segmented images are then processed using the GMM algorithm, which extracts key color characteristics. These characteristics include RGB and HSV values, color ratios, LAB color space information, Euclidean distances, and color co-occurrence frequencies. This comprehensive approach ensures a detailed and structured analysis of the color attributes present in Bonpo apparel and accessories.

Model validation with Bonpo apparel and accessories

To ensure the reliability and applicability of the developed color discrimination model regarding Bonpo apparel and accessories, this study conducts a multi-step validation process including accuracy validation and practical application potential validation. The validation of accuracy is conducted by t-test validation and expert evaluation. The practical application potential is conducted by color redesign toward Bonpo apparel.

T-test validation is achieved by comparing the RGB and HSV values of colors generated from datasets of different sizes. Specifically, after discriminating the color of Bonpo apparel and accessories regarding the full dataset, another part of dataset was randomly selected, and the same color discrimination method was applied. The extracted colors are then compared with those obtained from the full dataset. A t-test is conducted to evaluate the statistical differences between the RGB and HSV values of the two datasets, with the results determining whether the clustered colors remained consistent across different sample sizes.

Expert evaluation is conducted to assess the accuracy, fidelity, and cultural symbolism of the identified colors. In particular, accuracy refers to the precision with which the model detects and classifies the dominant colors present in the digital images of Bonpo heritage apparel and accessories. Fidelity reflects the degree of similarity between the colors identified by the model and the human-perceived original expression as judged by domain experts. Cultural symbolism refers to the extent to which the identified colors aligned with Bonpo cultural traditions. A panel of experts, including scholars specializing in religious clothing culture, Bon historians, and Tibetan traditional handicraft practitioners, are invited to provide assessments. Using a five-point Likert scale, they will rate the accuracy, fidelity and cultural symbolism regarding totally acceptable, acceptable, neutral, unacceptable, and totally unacceptable. In particular, totally acceptable reveals that the result is fully consistent with expert expectations. Acceptable infers to that the result is generally correct. Neutral refers to that the result is ambiguous or only partially aligned. Unacceptable indicates that the result shows clear inconsistencies or noticeable flaws that reduce its reliability. Totally unacceptable means that the result does not meet basic expectations and is not considered usable. To further refine the evaluation,

the entropy weight method is employed to quantify the relative importance of these criteria. This structured assessment ensures that the model not only captures the technical aspects of color identification but also maintains cultural authenticity, making it a valuable tool for analyzing heritage apparel.

Beyond the validation of accuracy, the model's practical application potential is examined through a color redesign for Bonpo apparel. A traditional Bonpo garment structure is selected, and a renewed color scheme is developed based on the extracted colors. The process involves analyzing the hues in HSV space to ensure diverse representation, selecting colors based on their ratio and co-occurrence patterns, and assigning them to specific garment regions in a balanced manner. Regarding the hue in HSV, colors from all hues should be considered. Regarding the color ratio and color co-occurrence frequency, the specific colors from each hue are selected. Within each hue, the color with the highest ratio is chosen as the primary color, and the color with the highest co-occurrence rate with the primary color is selected as the secondary. Then, the colors are assigned to the regions according to their ratios and the area of the region; the higher their ratios are, the larger the area of the region they will be filled in. Finally, a 3D model is generated to visualize the redesigned garment, demonstrating the model's effectiveness in guiding the application of color in traditional apparel. This highlights the model's capability not only to classify colors accurately but also to inform design decisions, making it a valuable tool for preserving and revitalizing cultural heritage through color analysis and application.

Results

Color discrimination model

The developed color discrimination model includes several sections with data acquisition, k determination, and color discrimination algorithm. In particular, the data acquisition section provides the necessary input for the model by collecting, improving, and segmenting images of heritage apparel and accessories. These segmented images serve as input for both the k determination and the color discrimination algorithm. In the k determination section, the segmented images are processed using the elbow method, which analyzes the SSE across different cluster numbers. This section determines the optimal k value, ensuring accurate color classification in the section of color discrimination algorithm. The color discrimination algorithm mainly includes the GMM to categorize colors into distinct clusters based on the segmented images and the optimal k value. The extracted color characteristics include RGB and HSV values, color ratios, LAB color space

information, Euclidean distances, and color co-occurrence frequencies, enabling a comprehensive and systematic analysis of heritage apparel colors.

Each section in this model is inherently interconnected. Accurate image segmentation directly influences the effectiveness of the GMM clustering, as well-segmented images improve the model's ability to analyze relevant regions. Likewise, the optimal k value determined by the elbow method ensures that the GMM effectively and objectively classifies colors. Finally, the color discrimination algorithm relies on GMM clustering results to generate meaningful color metrics. Together, these integrated sections form a robust and adaptable framework for accurately identifying and analyzing colors in heritage apparel and accessories. The overall structure of the color discrimination model is presented in Fig. 3.

Color discrimination for Bonpo apparel and accessories

More than 150 images were initially collected, and 86 images were qualified and were selected for the subsequent color discrimination. Examples of the selected images are present in Table 1.

Figure 4 is three samples of high-precision image restoration achieved using Bigjpg and Photoshop. In particular, Fig. 4(a) is a robe of monks wearing, Fig. 4(b) is costume wearing by performers in Bonpo ceremony, Fig. 4(c) apparel wearing by Bonpo masters. Figure 5(a)–(c) presents the FCM segmentation results of three samples toward the images in Fig. 4, respectively.

Figure 6 shows the SSE curves for the images in Fig. 5, with elbow points at $k = 2$, $k = 6$, and $k = 3$ for images Fig. 5(a)–(c), respectively. This suggests optimal cluster number of 2, 6, and 3, aligning with the colors in Bonpo apparel and accessories in Fig. 5.

By employing GMM, a color discrimination for Bonpo apparel and accessories was conducted. In particular, the names of the colors were assigned based on a comparison with the Pantone color system and references to daily regular names for the colors. Figure 7 presents the color clustering results for Fig. 5 based on the k values identified in Fig. 6. Figure 7(a) captures the dominant red and subtle orange of Fig. 5(a) in terms of their RGB or HSV. Similarly, Fig. 7(b) reflects the diverse colors in Fig. 5(b) based on their colors of RGB and HSV, including deep red, light beige, and warm beige, along with light taupe, light brown, and red. Figure 7(c) captures the deep red, light orange, and deep orange combination of Fig. 5(c). It is noted that with RGB and HSV, all colors can be identified with a specific color name.

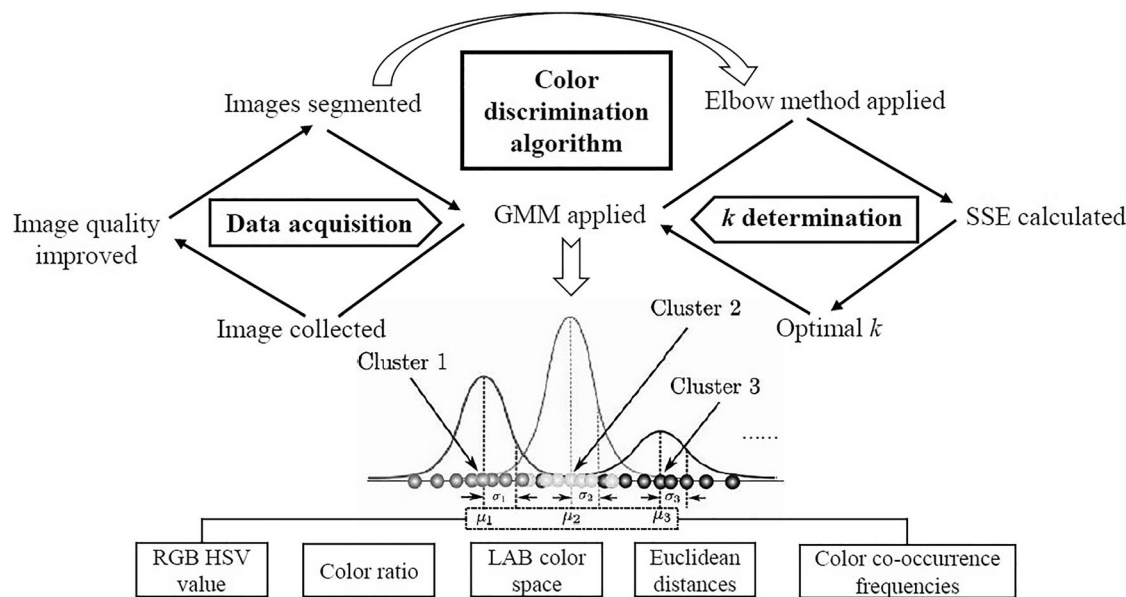


Fig. 3 | The overall structure of the color discrimination model.

Table 1 | Examples of the selected images for different characters

Location	Monks	Masters	Yogis	Performers	Priests
Yongzhong Lading Changdu Monastery					
Yongzhong Zuoqinling Temple					
Guangfa Temple					
Jiewayong Zhongdajiling Temple					
Museum					

Fig. 4 | Results of preprocessing for three samples.

a Robe of monks wearing, b costume wearing by performers in Bonpo ceremony, c apparel wearing by Bonpo masters.



(a) Robe of monks

(b) Bonpo ceremony costume

(c) Bonpo master apparel

Figure 8 shows the results of the initial GMM clustering toward all the 86 images. The wide range of identified colors indicates the complex palette in Bonpo apparel and accessories.

The above was the initial clustering of the images, and the second clustering was performed based on Fig. 8 to obtain the main colors of all 86 selected images of Bonpo apparel and accessories. Based on the expert panel method, this study decided to use the consensus-based values of $k = 10$ and $k = 20$ to achieve the second color clustering, respectively. In Table 2, the 10 clusters emphasize the dominant colors in terms of their RGB and HSV, such as reds, beiges, yellow, browns, taupe, and a single blue. These tones reflect the typical hues seen in the Bonpo apparel and accessories. The inclusion of blue and ochre yellow highlights colors associated with high-level masters' apparel and accessories. Table 3, with 20 clusters, captures additional subtle variations by breaking down dominant tones of Table 2

into smaller gradations, offering greater granularity for applications that require detailed color differentiation.

Table 4 presents the color ratios of the 10 main clustered colors from Table 2. The first 6 colors were primarily earthy tones, which aligns with the fact that Bonpos almost wear apparel and accessories that consist of color like beiges, taupes, browns, and reds⁴⁰. The last 4 colors in Table 4 are a mix of yellow, sienna red, and blue, providing vibrant and light accents that contrast with the muted tones.

The distribution of these 10 colors within the LAB color space is shown in Fig. 9. In terms of lightness (L*), Bonpo apparel and accessories fall between 10 and 80. Light beige has relatively high brightness values, while blue, reds, yellow, taupe, and browns range from 10 to 60. Dark brown, close to black, show the lowest brightness values. In terms of the red-green opponent channel (a*), most colors in Bonpo apparel and accessories are

Fig. 5 | Results of FCM segmentation for three samples. **a** FCM segmentation for the robe of monks wearing, **b** FCM segmentation for the costume wearing by performers in Bonpo ceremony, **c** FCM segmentation for the apparel wearing by Bonpo masters.

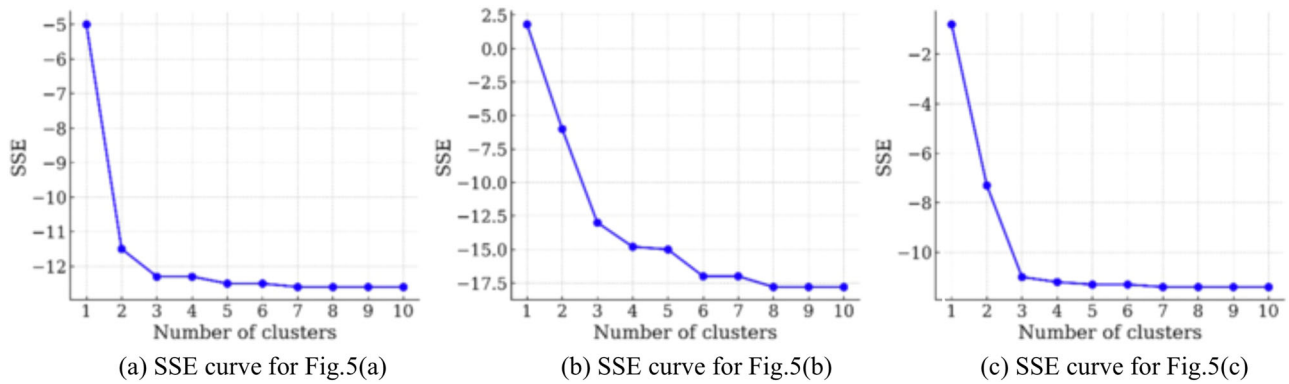


Fig. 6 | SSE curve for three samples. **a** SSE curve of Fig. 5(a) **b** SSE curve of Fig. 5(b) **c** SSE curve of Fig. 5(c).

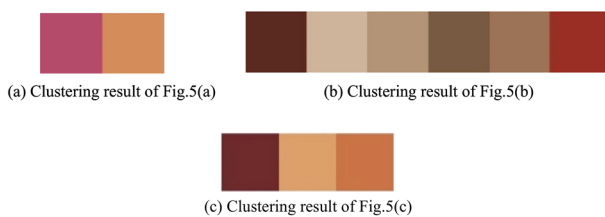


Fig. 7 | The clustering result for three samples. **a** Clustering result of Fig. 5(a) **b** Clustering result of Fig. 5(b) **c** Clustering result of Fig. 5(c).

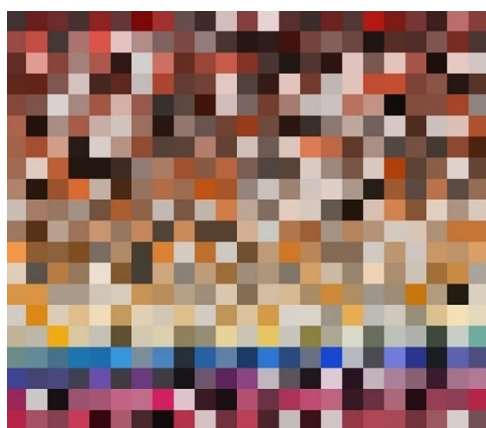
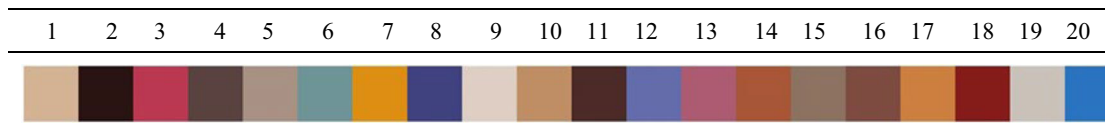


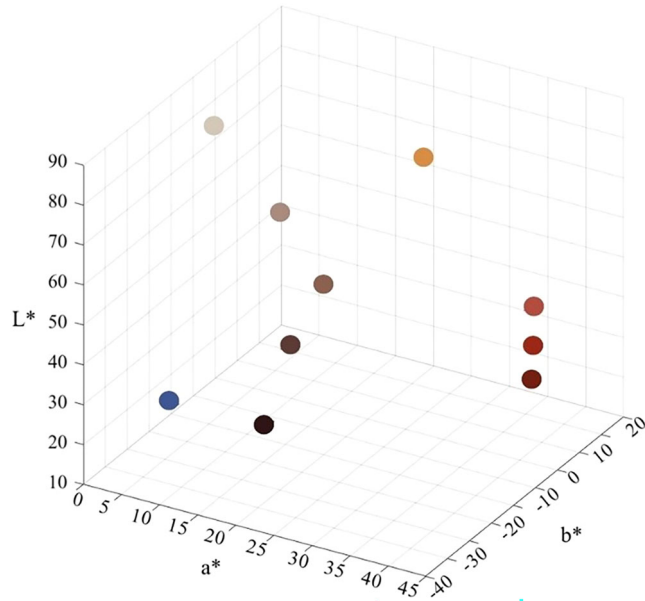
Fig. 8 | Results of the initial clustering for 86 images.

Table 2 | Colors in the second clustering with $k = 10$

No.	Color	Name	R	G	B	H (°)	S (%)	V
1		Warm beige	174	141	129	16	26	174
2		Deep red	100	34	31	3	69	100
3		Ochre yellow	206	138	73	29	65	206
4		Light beige	212	197	185	26	13	212
5		Sienna red	181	78	74	2	59	181
6		Dark brown	44	23	23	359	47	44
7		Cerulean blue	65	102	170	219	61	170
8		Light taupe	139	108	100	12	28	139
9		Rust brown	85	63	62	2	27	85
10		Mahogany	139	72	57	11	58	139

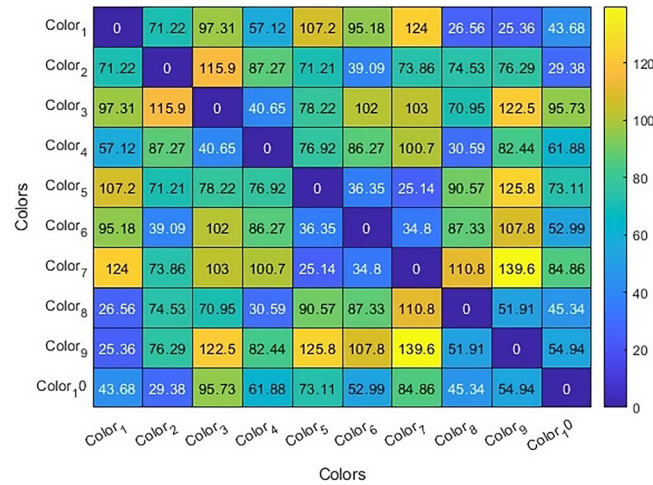
Table 3 | Colors of the second clustering with $k = 20$ **Table 4 | Color ratios of Bonpo apparel and accessories**

Name	Light beige	Warm beige	Mahogany	Dark brown	Rust brown
Color					
Ratio	0.206	0.120	0.120	0.110	0.106
Name	Light taupe	Ochre yellow	Sienna red	Deep red	Cerulean blue
Color					
Ratio	0.092	0.072	0.072	0.066	0.036

**Fig. 9 | LAB color space distribution.**

concentrated within a value of 15, while on the yellow-blue opponent channel (b^*), they primarily fall between 40 and 50.

As is demonstrated in the Fig. 10, colors that are closer to each other in the matrix (darker cells) share more similarity in terms of RGB. For example, the small distance between Color₁ (Warm beige) and Color₈ (Light taupe) (26.56) and Color₂ (Deep red) and Color₁₀ (Mahogany) (29.38) suggests these colors are quite similar. Large values such as Color₂ (Deep red) and Color₃ (Ochre yellow) with 115.9 or Color₇ (Cerulean blue) and Color₉ (Rust brown) with 139.6 indicate that these color pairs are quite different. Colors like Color₅ (Sienna red) and Color₆ (Dark brown) or Color₄ (Deep red) and Color₆ (Dark brown) have relatively small distances from each other, suggesting they belong to a similar color family. Color₄ (Light beige) shows higher distance values with many other colors, which might

**Fig. 10 | Color Euclidean distances matrix.**

indicate it represents a unique hue or significantly different tone from the rest.

Figure 11 displays the heatmap and data of color co-occurrence regarding the 10 main clustered colors in Table 2, highlighting high frequencies for Color₃ (Ochre yellow) with Color₇ (Cerulean) and Color₈ (Light taupe), at 0.6 and 0.7, respectively. These pairs likely represent well-coordinated color combinations in the image. The pair of Color₂ (Deep red) and Color₄ (Light beige) has a frequency of 0.01, indicating that they rarely appear together. Particularly, Color₃ (Ochre yellow) acts as a key connector color, with high co-occurrence across multiple pairs. It appears frequently with other neutrals and warm tones, such as Color₁ (Warm beige), Color₂ (Deep red), and Color₄ (Light beige), providing balance. In addition, the suggested color pairs align with the situation that collected images reflect, since the light beige, warm beige, and deep red are mostly used colors in the apparel and accessories worn by Bonpo covering all kinds of position and occasions.



Fig. 11 | Heatmap and the specific data of the co-occurrence.

Table 5 | The effectiveness of the GMM

Item	The first clustering	The second clustering
Average execution time/s	0.0185	6.2260
Average clustering error	0.5813	0.2907
Average silhouette score	0.5497	0.6366
Average DBI	0.5126	0.4378

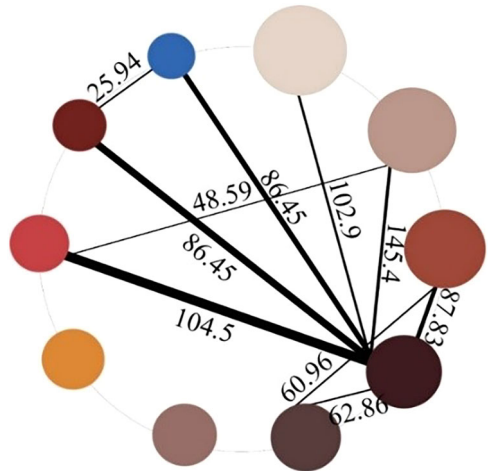


Fig. 12 | The color network for Bonpo apparel and accessories.

The average execution time, average clustering error and average silhouette score, and average Davies-Bouldin index (DBI) for the first clustering and the second clustering in GMM are presented in Table 5. It is noted that both clustering operations have relatively short execution times, the average clustering errors and DBI are low, the silhouette scores are high, indicating good performance in the clustering work.

In Fig. 12, the discriminated colors and their characteristics, such as color appearance, color ratios, co-occurrence frequency, and the Euclidean distances, are generated to build an overall color network for Bonpo apparel and accessories. First, the discriminated colors are arranged in a counter-clockwise direction based on their color ratios, with larger size color nodes representing higher color proportions. The thickness of the connecting lines between color nodes reflects the co-occurrence frequency, where higher co-

Table 6 | RGB and HSV values generated from 10 images

No.	Color	R	G	B	H (°)	S (%)	V
1		218	197	188	17	13	218
2		57	150	222	206	74	222
3		193	51	76	349	74	193
4		45	22	20	5	55	45
5		221	137	22	35	90	221
6		94	59	52	10	45	94
7		180	134	113	17	37	180
8		156	34	12	9	92	156
9		149	88	65	16	57	149
10		122	144	161	207	24	161

Table 7 | T-test results of RGB and HSV values

Channel	R	G	B	H	S	V
p-value	0.7401	0.8144	0.9293	0.7262	0.3104	0.4572

occurrence frequencies result in thicker lines. Particularly, the colors with co-occurrence frequency over 0.30 were generated to conduct the connecting lines³². The Euclidean distances are labeled near the lines, with larger values indicating greater spatial separation 6.

Model accuracy for Bonpo apparel and accessories

For the t-test validation, this study randomly selected 10 images of Bonpo apparel and accessories and introduced them to the previous color discrimination steps, and compare the RGB and HSV values of clustered colors from 86 and 10 images (Table 6). The results of t-test were demonstrated in Table 7, showing that all the p-values for the RGB and HSV channels are greater than 0.05, and indicating no significant differences in the means of the RGB and HSV channels between the two groups. This supports the conclusion that the two sets of colors are statistically similar in terms of their RGB and HSV values. Thus, the color discrimination model is valid.

Moreover, Table 8 shows the distribution of expert ratings for the accuracy, fidelity, and cultural symbolism of the identified Bonpo colors. The ratings indicate a strong consensus towards higher acceptability with 60%, 50%, and 60% experts, respectively. Table 9 presents the entropy weight and imply that for this evaluation, maintaining accurate color discrimination (42.036%) and ensuring cultural symbolism (26.026%) are more prioritized over the fidelity (31.938%). Table 10 displays the membership degrees and their normalized weights, it shows that “totally acceptable” and “acceptable” dominate the evaluation, and “Totally Acceptable” holds the highest normalized weight (0.412), followed by “Acceptable” (0.392). This indicates that higher levels of acceptability significantly influence the overall assessment.

Figure 13(a) and Fig. 13(b) are the selected structure of the front and back of regular apparel for divine dancers in Bon, respectively. Figure 14(a) presents the pattern of the structure in the Fig. 13, which suggests the area of each coloring regions. Figure 14(b) symmetrically demonstrated 1–7 labels for coloring regions according to the area of each region regarding the pattern presented in Fig. 14(a).

Table 8 | The statistics of the rating results

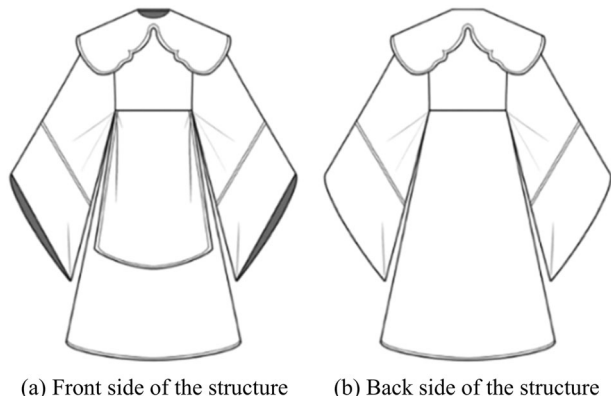
Item	Totally acceptable	acceptable	Neutral	Unacceptable	Totally unacceptable
Accuracy	0.6	0.4	0	0	0
Fidelity	0.5	0.3	0.2	0	0
Cultural symbolism	0.6	0.3	0.1	0	0

Table 9 | Entropy weight method calculation results

Item	Information entropy (e)	Information utility (d)	Weight
Accuracy	0.418	0.582	0.42
Fidelity	0.64	0.36	0.26
Cultural symbolism	0.558	0.442	0.32

Table 10 | Membership degree and normalized weight results

Item	Totally acceptable	acceptable	Neutral	Unacceptable	Totally unacceptable
Membership degree	0.420	0.400	0.200	0	0
Normalized membership degree	0.412	0.392	0.196	0	0

**Fig. 13 | The apparel structure to be colored. a** Front side of the structure **b** back side of the structure.

This study first analyzed the hue of the 10 colors using hue color wheel in Fig. 15. As is noted in Fig. 15 there is yellow hues consisting of light beige and warm beige, rust hues consisting of rust brown, light taupe and ochre yellow, red hues consisting of sienna red and deep red, and blue hues of cerulean blue. Then, this study determined the 7 colors from each hue for an even distribution. However, given that the blue hues contain only one color, this study incorporated two colors each from the yellow, rust, and red hues to achieve the desired balance in the color scheme. In the yellow hues, light beige and warm beige are selected. For the red hues, mahogany has the largest ratio, with dark brown as its highest co-occurring color. In the rust hues, rust brown holds the highest ratio, with ochre yellow as its closest match by co-occurrence, while cerulean blue represents the blue hues. Finally, the colors were assigned to the regions according to their ratios and the area of the region. Particularly, the yellow hues comprise 32.6% of the total, the rust hues 17.8%, the red hues 23%, and the blue hues 3.6%. Following this distribution, colors are accordingly applied first in the regions of the apparel structure. Based on these steps, the color design scheme was developed and presented in the Table 11. The 3D model of the color design result regarding the Bonpo apparel in Fig. 11 is presented in Fig. 16.

Discussion

In this paper, the computational algorithms including FCM, Elbow method, and GMM were applied to develop a color discrimination model for heritage apparel and accessories, and introduce Bonpo apparel and accessories as case study to validate the model. This color discrimination model with color characteristics of color ratios, LAB color space, color Euclidean distance, and color co-occurrence frequency, accurately discriminated the color of heritage apparel and accessories. Moreover, the objective validation regarding t-test, subjective validation regarding expert panel, and color redesign application were conducted to validate the accuracy and applicable potential of the model.

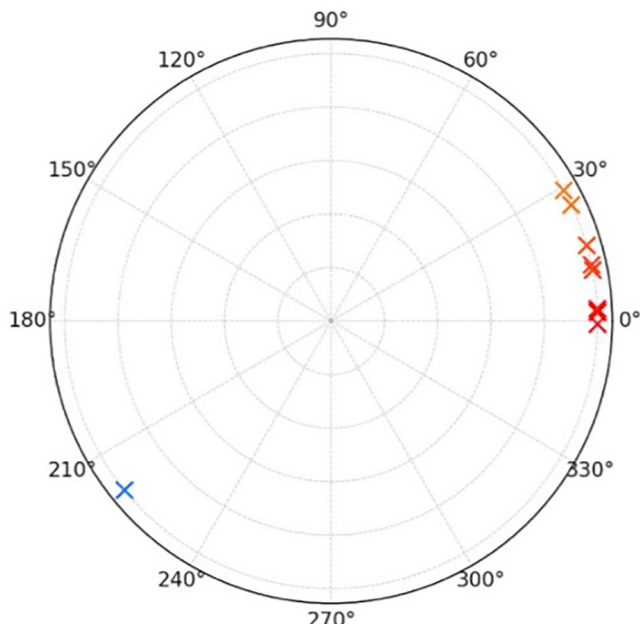
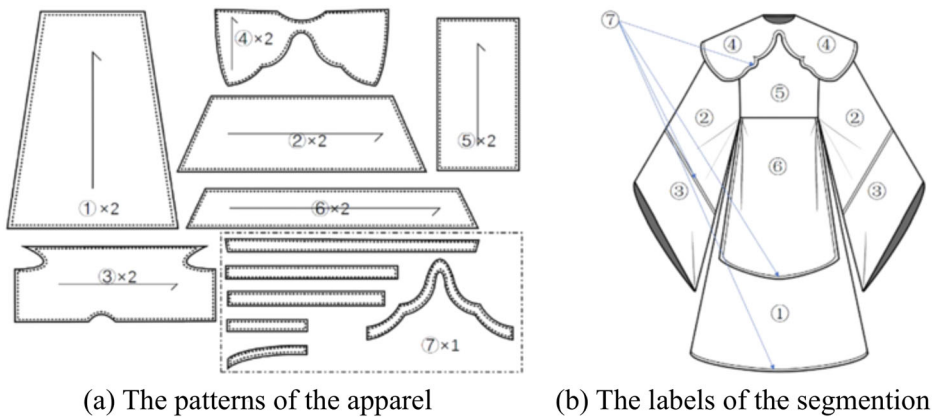
The following conclusions can be drawn from the results: (1) even with limited and low-quality resources and complex color compositions regarding monochromatic schemes and polychromatic schemes, the computational algorithm-based color discrimination model can accurately, systematically, and comprehensively identify the color characteristics of heritage apparel and accessories. (2) The results from this model can provide valuable data support for the application and redesign of the colors regarding heritage apparel and accessories.

The main contributions of this study are as follows: (1) the developed color discrimination model enables more accurate and efficient analysis of heritage apparel and accessories' colors, supporting further theoretical research on color-related cultural heritage and design; (2) this model provides a practical tool for the digital preservation, restoration, and innovative utilization of heritage apparel and accessories regarding color characteristics, facilitating accurate its application in museum and contemporary fashion design.

The work nevertheless has some limitation and deserve further discussion. The first limitation is that the model relies heavily on centralized clustering assumptions as GMM's Gaussian distributions, which may oversimplify color distributions in few heritage apparel and accessories with non-linear or fragmented patterns as degraded dyes or mixed materials. Future work could integrate non-parametric clustering algorithm to address this. The second limitation is that the study only focuses on typical datasets and scenario, which may not fully reflect the applicability of this study on the overall heritage apparel and accessories. Future work could expand datasets to unearthed heritage apparel and accessories and more scenarios across multiple heritage apparel and apparel besides Bonpo garment. Moreover, future work could further implement Machine Learning (ML) and other techniques

Fig. 14 | The segmentation for coloring regions.

a The pattern of the apparel b The labels of segmentation.

**Fig. 15 | The hue color wheel of the Bonpo apparel and accessories.****Table 11 | The color scheme of for the apparel**

No.	Color	Name	Ratio	H (°)	S (%)	V
4		Light beige	0.206	26	13	212
1		Warm beige	0.120	16	26	174
2		Deep red	0.120	3	69	100
6		Dark brown	0.110	359	47	44
9		Rust brown	0.106	2	27	85
3		Ochre yellow	0.072	29	65	206
7		Cerulean blue	0.036	219	61	170

to process the image data and develop adaptive algorithms for theme color extraction and context-aware palette generation tailored to cultural aesthetics.

Data availability

The image data used and analyzed during the current study are not publicly available due to participant privacy concerns. However, anonymized or representative processed data may be available from the corresponding author upon reasonable request and with appropriate ethical clearance.

Received: 17 January 2025; Accepted: 4 June 2025;

Published online: 21 June 2025

References

1. Hertz, C. Dressing the part: producing ethnic minority textiles in the era of intangible cultural heritage tourism. *J. Ethnol. Folkloristics* **18**, 90–122 (2024).
2. Lan, L. & Liu, P. Changing identity in Chinese fashion: Self-choice and preference during late Qing Dynasty and Republican China. *Textile* **22**, 681–702 (2024).
3. Liu, Y. & Zhang, Y. W. Quilted Kasaya in seven strips of mottled colors contained in Todai-ji Kenmotsu Cho. *Basic Sci. J. Text. Univ.* **37**, 111–117 (2024).
4. El Azhar, S. The changing roles of female visual artists in Morocco. *J. Glob. Initiat. Policy, Pedagog., Perspect.* **14**, 6 (2019).

**Fig. 16 | Color design for the apparel of divine dancer.**

5. Zhang J., Miller A. H. D. & Westerhof Nyman P. J. Creating authentic historical costumes to augment virtual humans for cultural heritage. Immersive Learning Research Network, (2025).
6. Franceschini, M. Navigating fashion: on the role of digital fashion archives in the preservation, classification and dissemination of fashion heritage. *Crit. Stud. Fash. Beauty* **10**, 69–90 (2019).
7. Lu, Z., Huang, X. & Mei, Y. J. Digital innovation design and application Han dynasty inscriptions brocade. *Basic Sci. J. Text. Univ.* **36**, 51–59 (2023).
8. Hu, W. & Zhang, Y. Application of image colour matching algorithm based on visual perception model in clothing design. *Int. J. Inf. Commun. Technol.* **25**, 16–24 (2024).
9. Tena, S., Hartanto, R. & Ardianto, I. Content-based image retrieval for fabric images: a survey. *Indones. J. Electr. Eng. Comput. Sci.* **23**, 1861 (2021).
10. Kottangal A. & Purohit D. The significance of Lakiya Negev Bedouin heritage weave—a way of knowing Israel's cultural costume. *Journal of Cultural Heritage Management and Sustainable Development*, (2024).
11. Carrillo-Perez, F. et al. Applications of artificial intelligence in dentistry: A comprehensive review. *J. Esthet. Restor. Dent.* **34**, 259–280 (2022).
12. Becker, C. J. & Nowak, B. Iklan Aesthetics in Niger: Identity and Adornment from Servility to Self-agency. *Afr. arts* **55**, 10–25 (2021).
13. Tamburini, D. et al. An introduction and recent advances in the analytical study of early synthetic dyes and organic pigments in cultural heritage. *Heritage* **7**, 1969–2010 (2024).
14. Kværne P. A. Glimpses of Tibetan Divination. 1st ed. Netherland: Brill, (2019).
15. Zhao, S. et al. Examination of Digitalized Non-Heritage Apparel Design Using CLO3D: Case Study of Ningbo Gold and Silver Color Embroidery. *Valley International Journal Digital Library*, 19–32 (2024).
16. Cho, H. Y. The Language of Miao Embroidery: Exploring the Traditional “Embroidered Rear Skirt Panels” Worn by the Miao Women of the Huawu Village. *Textile* **21**, 2–31 (2023).
17. Celani, C. P. et al. Exploring elucidation of red dye mixtures on woolen historical textiles via non-destructive spectroscopic analysis and multivariate cluster analysis. *Herit. Sci.* **12**, 48 (2024).
18. Kaplan, G. & Seferoglu, Z. The synthetic approaches for preparation of indigo and applications in denim industry. *Curr. Org. Synth.* **20**, 361–364 (2023).
19. Dorozynski, M. & Rottensteiner, F. Deep descriptor learning with auxiliary classification loss for retrieving images of silk fabrics in the context of preserving European Silk Heritage. *ISPRS Int. J. Geo-Inf.* **11**, 82 (2022).
20. Zhao, L., Wang, Z., Zuo, Y. & Hu, D. Comprehensive evaluation method of ethnic costume color based on k-means clustering method. *Symmetry* **13**, 1822 (2021).
21. Gogebakan, M. A novel approach for Gaussian mixture model clustering based on soft computing method. *IEEE Access* **9**, 159987–160003 (2021).
22. Cerrillo-Cuenca, E. et al. Color-based discrimination of color hues in rock paintings through Gaussian mixture models: a case study from Chomache site (Chile). *Herit. Sci.* **12**, 169 (2024).
23. Intharah, T. & Khiripet, N. MuralCut: automatic character segmentation from mural images. 2012 9th International Conference on Electrical Engineering/Electronics, Computer, Telecommunications and Information Technology. 1–4 (IEEE, 2012).
24. Zhou, S. & Xie, Y. Intelligent restoration technology of mural digital image based on machine learning algorithm. *Wirel. Commun. Mob. Comput.* **2022**, 4446999 (2022).
25. Xia, D. H. et al. Material degradation assessed by digital image processing: Fundamentals, progresses, and challenges. *J. Mater. Sci. Technol.* **53**, 146–162 (2020).
26. Enninful, E. K., Boakye-Amponsah, A. & Vanderpuye, P. An empirical analysis of technology-induced image fading in digital prints among photography students. *Int. J. Innov. Creat. Chang.* **17**, 53–81 (2023).
27. Zhiwei, H. et al. The digital restoration of ladies' costumes in the palace music chart. *J. Text. Res.* **45**, 155–164 (2024).
28. Yang, X. et al. Fuzzy c-multiple-means clustering for hyperspectral image. *IEEE Geosci. Remote Sens. Lett.* **20**, 1–5 (2023).
29. Sutomo, F. et al. Optimization of the k-nearest neighbors algorithm using the elbow method on stroke prediction. *J. Tek. Inform.* **4**, 125–130 (2023).
30. Zhang, J. & Liu, C. A study of a clothing image segmentation method in complex conditions using a features fusion model. *Automatika* **61**, 150–157 (2020).
31. Malhotra, J. & Jha, S. Fuzzy c-means clustering based colour image segmentation for tool wear monitoring in micro-milling. *Precis. Eng.* **72**, 690–705 (2021).
32. Hung, W. L., Yang, M. S. & Chen, D. H. Bootstrapping approach to feature-weight selection in fuzzy c-means algorithms with an application in color image segmentation. *Pattern Recognit. Lett.* **29**, 1317–1325 (2008).
33. Patel, E. & Kushwaha, D. S. Clustering cloud workloads: K-means vs Gaussian mixture model. *Procedia Comput. Sci.* **171**, 158–167 (2020).
34. Hajhosseini, M., Maghsoudi, A. & Ghezelbash, R. A comprehensive evaluation of OPTICS, GMM and K-means clustering methodologies for geochemical anomaly detection connected with sample catchment basins. *Geochemistry* **84**, 126094 (2024).
35. Sugiharto, N. D. et al. Mall customer clustering using Gaussian mixture model, K-means, and BIRCH algorithm. 2023 6th International Conference on Information and Communications Technology (ICOIACT). 212–217 (IEEE, 2023).
36. Widiono, S., Noersasongko, E. & Soeelman, M. A. Segmentation of Stacked Leaf Images for Enhanced Visual Monitoring Using Gaussian Mixture Models (GMM) Algorithms. 2023 6th International Seminar on Research of Information Technology and Intelligent Systems (ISRITI). 59–64 (IEEE, 2023).
37. Hanif, M. et al. Restoration and content analysis of ancient manuscripts via color space-based segmentation. *Plos one* **18**, e0282142 (2023).
38. Rafid, M. et al. The effect of LAB color space with NASNetMobile fine-tuning on model performance for crowd detection. *Adv. Sustain. Sci. Eng. Technol.* **6**, 02401014 (2024).
39. Ryavec, K. E. Regional Perspectives on the Origin and Early Spread of the Bon Religion based on Core Areas of Monastery Construction across the Tibetan Plateau. *Revue d'Etudes Tibétaines*, 5 (2020).
40. Schneider, N. A revolution in red robes: Tibetan nuns obtaining the doctoral degree in buddhist studies (Geshema). *Religions* **13**, 838 (2022).

Acknowledgements

This research was funded by the Chongqing Federation of Social Sciences (Grant No. 2024NDYB179).

Author contributions

Conceptualization: Yu Zhao and Yi Xiang; investigation: Yu Zhao and Yan Cheng; data preparation: Yan Cheng; analysis and software: Yan Cheng and Yuxiang Zhang. All authors read and approved the final manuscript.

Competing interests

The authors declare no competing interests.

Additional information

Correspondence and requests for materials should be addressed to Yi Xiang.

Reprints and permissions information is available at

<http://www.nature.com/reprints>

Publisher's note Springer Nature remains neutral with regard to jurisdictional claims in published maps and institutional affiliations.

Open Access This article is licensed under a Creative Commons Attribution-NonCommercial-NoDerivatives 4.0 International License, which permits any non-commercial use, sharing, distribution and reproduction in any medium or format, as long as you give appropriate credit to the original author(s) and the source, provide a link to the Creative Commons licence, and indicate if you modified the licensed material. You do not have permission under this licence to share adapted material derived from this article or parts of it. The images or other third party material in this article are included in the article's Creative Commons licence, unless indicated otherwise in a credit line to the material. If material is not included in the article's Creative Commons licence and your intended use is not permitted by statutory regulation or exceeds the permitted use, you will need to obtain permission directly from the copyright holder. To view a copy of this licence, visit <http://creativecommons.org/licenses/by-nc-nd/4.0/>.

© The Author(s) 2025